RSC Advances

ROYAL SOCIETY OF CHEMISTRY

www.rsc.org/advances

Cite this: DOI: 10.1039/c0xx00000x

www.rsc.org/xxxxxx

ARTICLE TYPE

The reactivity of *o*-amidophenolate indium(III) complexes towards different oxidants

Alexandr V. Piskunov,*[a,b] Irina N. Meshcheryakova,[a] Irina V. Ershova,[a] Artyem S. Bogomyakov,[c] Anton V. Cherkasov[a] and Georgy K. Fukin[a,b]

Received (in XXX, XXX) Xth XXXXXXXXX 20XX, Accepted Xth XXXXXXXXX 20XX
DOI: 10.1039/b000000x

The reactivity of *o*-amidophenolate indium(III) complexes towards different oxidants was investigated. The oxidation reactions were found to proceed through the stage of paramagnetic *o*-iminobenzosemiquinonato indium(III) derivative formation. The monoradical intermediates undergo the symmetrization. The final products of oxidation processes are corresponding biradical *o*-iminobenzosemiquinonato indium(III) complexes. In order to understand the reasons of the symmetrization processes sterical factors (G-parameters) were evaluated for all intermediates and final products by method based on the ligand solid angle approach.

Introduction

It is well known that the chemical properties of organometallic and coordination compounds are determined by the nature of metal center and the peculiarities of ligand molecular and electronic structure. The variation of metal and ligand nature allows to modify finely the reactivity of coordination compounds and create the most effective reagents. The participation of such type ligands in redox processes enables the realization of various unique transformations of main group element compounds. The abilities of such complexes to the reversible binding of small molecules (dioxygen [1], nitrogen monoxide [2]) and the activation of triple C≡C bonds of terminal alkynes [3] or C-Hal bonds of alkyl halides [4] are examples of transition metal chemistry acquisition realized by the main group metal compounds. It allows to involve the nontransition metal complexes into the various relevant chemical transformations in particular catalytic processes [5].

The diverse chemistry of transition metal complexes based on *o*-quinone type ligands is under wide investigations in a number of research groups and collected in reviews and recent papers [6]. The data concerning such nontransition metal derivatives are quite scarce. The nontransition metal compounds based on dianions of *o*-quinone type redox active ligands (substituted *o*-benzoquinones and *o*-iminobenzoquinones) are known to react readily with different oxidants [7] (O-, N-, S-, C-centered radicals, dioxygen, sulfur, halogens, etc.). The paramagnetic radical anion (*o*-benzosemiquinonate or *o*-iminobenzosemiquinonate) metal complexes form as a result. These compounds can be detected by EPR spectroscopy. The stability of such paramagnetic species was found to depend on the electronic and sterical effects of substituents bound to metal as well as solvent nature [8]. The unstable derivatives undergo a symmetrization or reductive elimination of hydrocarbon fragment [7h, 8, 9]. For example, the monoradical indium(III) derivatives based on 3,6-di-*tert*-butylcatecholate ligand can be prepared by the oxidation of corresponding diolate complexes. The detected paramagnetic species are unstable and undergo the subsequent transformations [9]. Recent investigations have shown that the indium(III) complexes can involve all three possible redox forms of the *o*-iminobenzoquinone ligand depending on the coordination environment of metal [10]. The present study is devoted to the investigation of reactivity of *o*-amidophenolate indium(III) complexes APInI(TMEDA) (**1**) and $[APInEt]_2$ (**2**) (where AP is 4,6-di-tert-butyl-*N*-(2,6-diisopropylphenyl)-*o*-amidophenonate dianion, TMEDA is *N,N,N'N'*-tetramethylethylenediamine) towards different oxidants.

Results and discussion

Reactions of *o*-amidophenolate indium(III) complexes 1 and 2 with different oxidants: Characterization of the products.

The objects of presented investigation are the recently described *o*-amidophenolate indium(III) complexes APInI(TMEDA) (**1**) and $[APInEt]_2$ (**2**) [10b]. Both of these compounds are tested in the reactions with different oxidative agents (iodine, mercury(II) chloride, tetramethylthiuramedisulphide (TMUDS) and dioxygen) (Schemes 1-3). All interactions are completed in few minutes and accompanied by the change of colour of reaction mixture from orange (for **1**) or pale yellow (for **2**) to deep green indicating the oxidation of *o*-amidophenolate ligand into *o*-iminosemiquinolate one.

The *o*-amidophenolate antimony complexes are known to be reactive towards dioxygen. These reactions occur at mild conditions and result in the formation of corresponding metal containing endoperoxides [1]. In contrast to such reactivity, complex **1** reacts with dioxygen and gives paramagnetic

Cite this: DOI: 10.1039/c0xx00000x

www.rsc.org/xxxxxx

ARTICLE TYPE

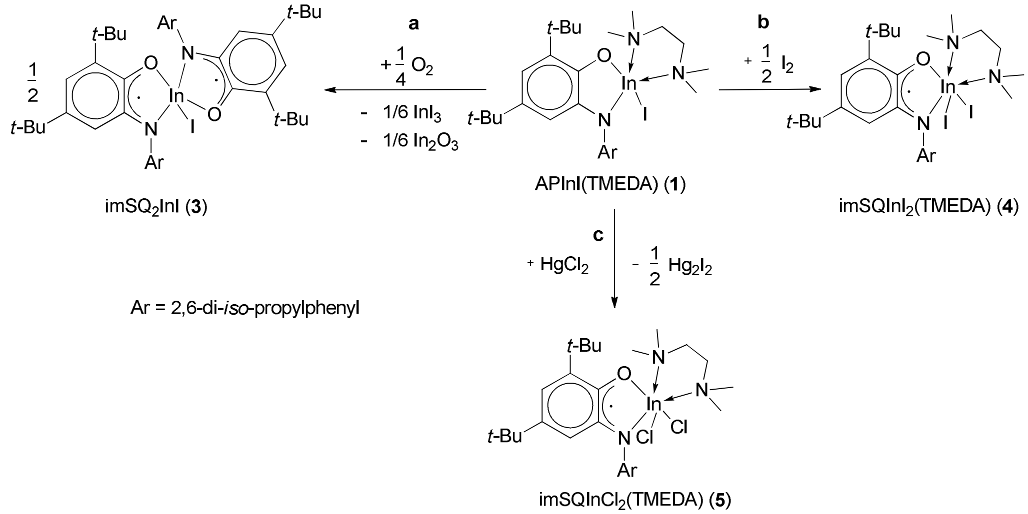

Scheme 1. The interaction of **1** with dioxygen (a), iodine (b) and $HgCl_2$ (c)

derivative as a final product. It was identified as known [10a] *o*-iminobenzosemiquinonato indium(III) complex imSQ$_2$InI (**3**) (where imSQ - 4,6-di-tert-butyl-*N*-(2,6-diisopropylphenyl)-*o*-iminosemiquinonate ligand) in the accordance with IR-, EPR spectroscopy and elemental analysis (Scheme 1, path **a**). Such behaviour is very similar to that observed for tin(IV) *o*-amidophenolates [7h]. The oxidation of **1** with iodine leads to the formation of another known [10b] *o*-iminobenzosemiquinonato indium(III) complex imSQInI$_2$(TMEDA) (**4**) (Scheme 1, path **b**). The interaction of **1** with $HgCl_2$ is accompanied with halogen exchange process (Scheme 1, path **c**). Instead of an expected mixed-halogen derivative, the indium(III) compound imSQInCl$_2$(TMEDA) (**5**) containing two chlorine atoms bound to the metal centre forms as the result. The presumable driving force for the additional halide exchange is the lower solubility of mercury(I) iodide versus respective chloride [11]. The molecular structure of the later was confirmed by X-ray diffraction analysis.

Complex **5** is paramagnetic both in solution and in solid state. The hyperfine structure of X-band EPR spectrum registered in THF (Fig. 1) at 290 K is caused by the interaction of unpaired electron with magnetic nuclei of *o*-iminobenzosemiquinonato ligand (^{1}H, 99.98%, I = 1/2, μ_N = 2.7928 and ^{14}N, 99.63%, I = 1, μ_N = 0.4037 [12]), metal centre (^{113}In, 4.3%, I = 9/2, μ_N = 5.229 and ^{115}In, 95.7%, I = 9/2, μ_N = 5.534 [12]), one of the halogen substituents (^{35}Cl, 75.77%, I = 3/2, μ_N = 0.8218 and ^{37}Cl, 24.23%, I = 3/2, μ_N = 0.6841 [12]) and one of the nitrogen atoms of TMEDA molecule. The splitting parameters are the following: $a_i(^{1}H)$ = 4.8 G, $a_i(^{14}N)$ = 7.4 G, $a_i(^{113}In)$ = 12.5 G, $a_i(^{115}In)$ = 13.2 G, $a_i(^{35}Cl)$ = 0.8 G, $a_i(^{37}Cl)$ = 0.7 G, $a_i(^{14}N)$ = 1.1 G (g_i = 2.0024).

The interaction of APInI$_2$(TMEDA) (**1**) with TMUDS is also completed during few minutes at moderate heating (40-50ºC) and proceeds through the formation of monoradical *o*-iminobenzosemiquinonato species imSQInI(SS)(TMEDA) (**8**) at the first stage (Scheme 2, path **a**).

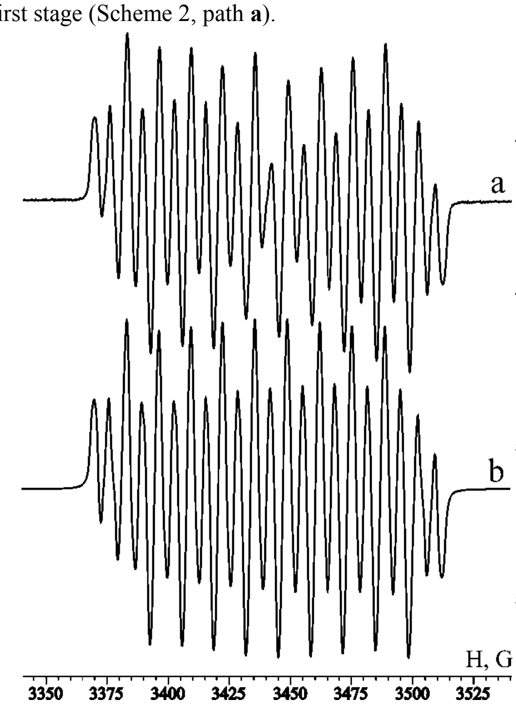

Fig. 1. The X-band EPR spectrum of **5** in THF at 290 K. a – experimental, b – simulated

The reaction mixture (THF solution at 290K) is characterized by well resolved EPR spectrum. The hyperfine structure is caused by the interaction of unpaired electron with magnetic nuclei of redox active ligand and metal centre. The splitting parameters are: $a_i(^{1}H)$ = 4.9 G, $a_i(^{14}N)$ = 6.4 G, $a_i(^{115}In)$ = 12.3 G, $a_i(^{113}In)$ = 11.6 G (g_i = 2.0026). It is reasonable to assume that this paramagnetic

Cite this: DOI: 10.1039/c0xx00000x

www.rsc.org/xxxxxx

ARTICLE TYPE

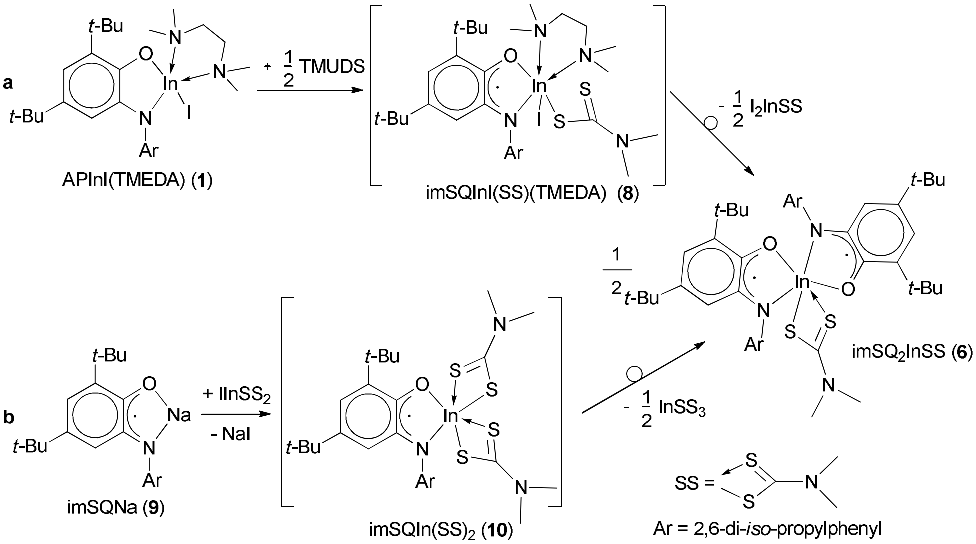

Scheme 2. The preparation of complex imSQ$_2$InSS (**6**)

product is imSQInI(SS)(TMEDA) (**8**). We can not unambiguously ascertain the coordination environment of metal centre in this monoradical *o*-iminobenzosemiquinonato indium(III) derivative **8**. The TMEDA molecule and dithiocarbamate ligand can be either mono- or bidentate bound to indium atom. But it is known [6f] that the value of hyperfine splitting constants on metal magnetic isotopes in the EPR spectra for the related compounds depends on the metal coordination number: it decreases with increasing coordination number. The value of splitting parameter $a_i(^{115}In)$ of observed EPR spectrum (12.3 G) for **8** is slightly less than that parameter for complex **5** ($a_i(^{115}In)$ = 13.2 G). It indicates that the value of coordination number of the metal centre in imSQInI(SS)(TMEDA) is equal six or more. The intensity of observed isotropic EPR signal decreases until full disappearance during two hours and the biradical complex **6** forms as the result (Scheme 2, path **a**). Apparently the second product of symmetrization is dithiocarbamate indium(III) diiodide I_2InSS which precipitates from the reaction mixture as white powder.

The compound imSQ$_2$InSS (**6**) containing two *o*-iminobenzosemiquinonato and one dithiocarbamate ligands is the fine-crystalline dark green solid. The EPR spectrum of **6** in toluene matrix at 150 K is typical for biradical species and the half-field signal (Δm_s = 2) is observed as well. However both signals (Δm_s = 1 and Δm_s = 2) are significantly broadened and the clear determination of zero-splitting parameters is impossible. The broadening can be explained by the presence of additional line splitting on the indium magnetic nuclei.

As mentioned above the intermediate monoradical *o*-iminobenzoquinonato indium(III) species containing dithiocarbamate ligand imSQInI(SS)(TMEDA) (**8**) is unstable

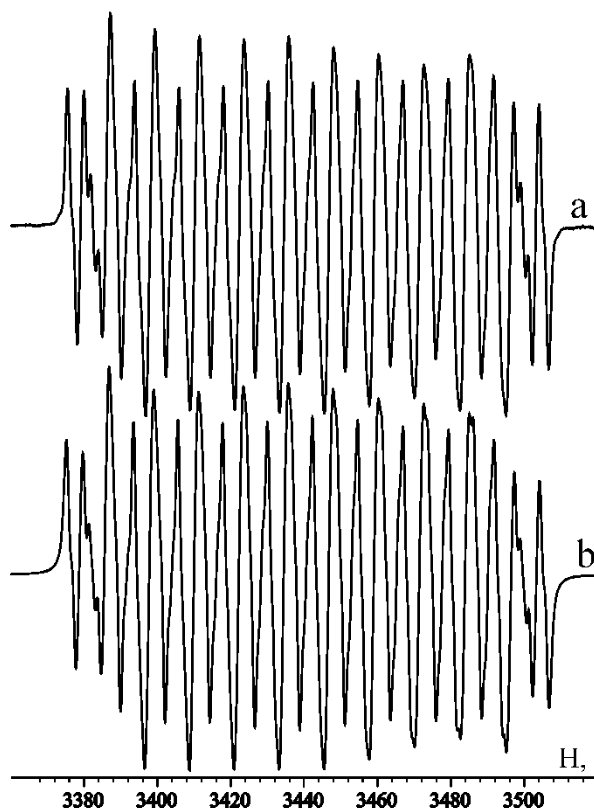

Fig. 2. The X-band EPR spectrum of imSQInSS$_2$ (**10**) in toluene at 290 K. a – experimental, b – simulated

and undergoes symmetrization. We have made an attempt to obtain monoradical indium(III) derivative containing two dithiocarbamate ligands by the exchange reaction of

Cite this: DOI: 10.1039/c0xx00000x

www.rsc.org/xxxxxx

ARTICLE TYPE

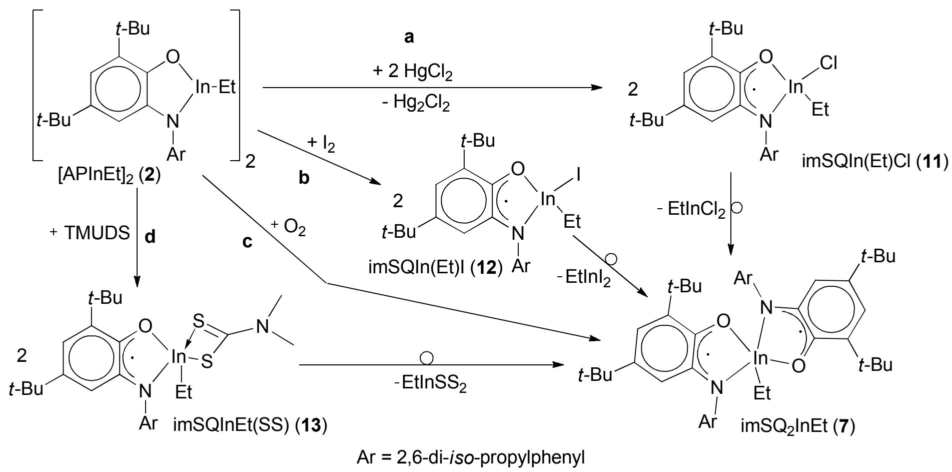

Scheme 3. The interaction of **2** with $HgCl_2$ (a), I_2 (b), O_2 (c) and TMUDS (d)

sodium *o*-iminosemiquinolate (**9**) with $IInSS_2$ (Scheme 2, path **b**). The expected mono-*o*-iminobenzosemiquinonato indium(III) species $imSQInSS_2$ (**10**) forms as an intermediate product on the first stage and was detected using EPR technique. The reaction mixture demonstrates isotropic EPR spectrum in toluene at 290 K (Fig. 2). Its hyperfine structure is caused by the interaction of unpaired electron with magnetic nuclei of the redox active ligand and metal centre. It should be noted that we were able to observe the splitting relating to the proton at carbon atom C(5) of imSQ ligand in the EPR spectrum in the case of $imSQInSS_2$ (**10**). Usually one cannot observe this kind of hyperfine interaction due to the great line width (2-3 G). The splitting parameters are following: $a_i(^1H)$ = 4.4 G, $a_i(^1H)$ = 1.4 G, $a_i(^{14}N)$ = 6.9 G, $a_i(^{115}In)$ = 12.3 G, $a_i(^{113}In)$ = 11.6 G (g_i = 2.0027). The biradical compound **6** was also isolated as the final product of this reaction (Scheme 2, path **b**).

The interaction of indium(III) amidophenolate complex $[APInEt]_2$ (**2**) with iodine, mercury(II) chloride and TMUDS also proceeds through the stage of paramagnetic mono-*o*-iminobenzosemiquinonato indium(III) species (**11-13**) formation (Scheme 3, path **a**, **b** and **d**). Each of the derivatives formed was characterized by EPR spectroscopy. The hyperfine structure of EPR signals observed is caused by the interaction of unpaired electron with magnetic nuclei of redox active ligand, metal centre and halogen nuclei (in the case of imSQIn(Et)I (**12**) and imSQIn(Et)Cl (**11**)). The splitting parameters are the following: $a_i(^1H)$ = 4.2 G, $a_i(^{14}N)$ = 6.7 G, $a_i(^{115}In)$ = 22.9 G, $a_i(^{113}In)$ = 21.6 G, $a_i(^{127}I)$ = 0.5 G (^{127}I, 100%, I = 5/2, μ_N = 2.808 [12]), g_i = 2.0021 for imSQIn(Et)I (**12**) (pentane, 290 K); $a_i(^1H)$ = 4.6 G, $a_i(^{14}N)$ = 6.6 G, $a_i(^{115}In)$ = 23.0 G, $a_i(^{113}In)$ = 21.7 G, $a_i(^{35}Cl)$ = 0.8 G, $a_i(^{37}Cl)$ = 0.7 G, g_i = 2.0025 for imSQIn(Et)Cl (**11**)(THF, 290 K); $a_i(^1H)$ = 4.6 G, $a_i(^{14}N)$ = 6.5 G, $a_i(^{115}In)$ = 19.1 G, $a_i(^{113}In)$ = 18.1 G, g_i = 2.0024 for imSQInEt(SS) (**13**) (THF, 290 K). The EPR spectrum of imSQIn(Et)I (**12**) in pentane at 290 K is presented on Figure 3.

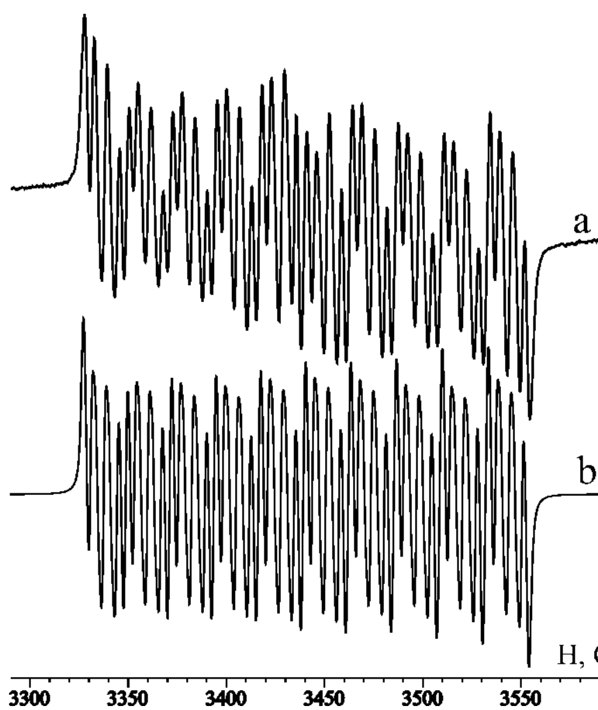

Fig. 3. The X-band EPR spectrum of imSQIn(Et)I (**12**) in pentane at 290K. a – experimental, b – simulated

It should be noted that the value of the hyperfine splitting constant $a_i(^{115}In)$ characteristic for intermediate oxidation products (**11-13**) of complex **2** exceeds twice the corresponding parameter for analogous derivatives (**8, 10**) formed as the result of the oxidation of compound **1**. It indicates the differences in the coordination centre geometry of intermediate products. The coordination number for derivatives **11-13** is less than that for **8, 10** and equals four (**11, 12**) or five (**13**).

The intensity of isotropic EPR signals of **11-13** decreases in time and the spectrum typical for biradical appears in frozen solvent matrix at 150 K. Indeed the final product for any redox reaction (Scheme 3) is compound **7** containing two *o*-iminobenzosemiquinonato ligands and ethyl group at indium atom. Thus the mono-*o*-iminobenzosemiquinonato indium(III) derivatives undergo the symmetrization (Scheme 3, path **a**, and **d**). The co-products of this symmetrization are $EtInCl_2$, $EtInI_2$ and $EtInSS_2$ (for the path **a**, **b** and **d** respectively). The oxidation of **2** with dioxygen also leads to complex **7** (Scheme 3, path **c**), however we were unable to register any intermediate products of this reaction.

Complex **7** was characterized by EPR spectrum typical for biradical species (Fig. 4). As in the case of $imSQ_2InSS$ (**6**), the signal shown on Figure 4 is significantly broadened due to the hyperfine interaction of radical centers with indium magnetic nuclei. Therefore we were unable to determine precisely the zero-splitting parameters.

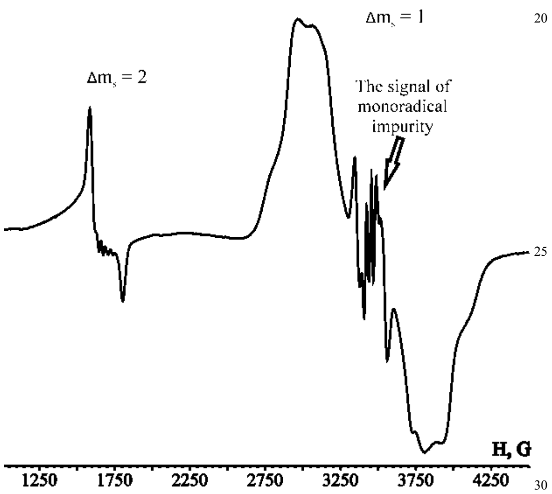

Fig. 4. The EPR spectrum of $imSQ_2InEt$ (**7**) in toluene matrix at 150 K

Magnetic properties of complexes 6 and 7.

The magnetochemical investigations for biradical complexes **6** and **7** were performed. The quite different behaviour was observed as a result. Temperature dependences of the effective magnetic moments (μ_{eff}) are presented in Figure 5. The value of μ_{eff} at 300 K (2.39 and 2.44 μ_B for **6** and **7** respectively) is close to spin-only value 2.45 μ_B typical for system with two non-interacting paramagnetic centres with S = 1/2.

At lowering temperature the μ_{eff} value of complex **6** decreases insensibly in the range 300-80K and more suddenly below 80 K and reaches 0.92 μ_B at 5 K. It indicates the domination of antiferromagnetic exchange interactions between unpaired electrons of *o*-iminobenzosemiquinonato ligands. Exchange coupled dimer model ($H = -2JS_1S_2$) describes experimental data poorly (Figure 5, dotted line). Indeed in accordance with X-ray diffraction data the molecules of **6** are packed as in chains, and there are the short C…H contacts (2.7-2.8 Å) between hydrogen atoms of *tert*-butyl groups of one molecule and carbon atoms of aryl substituent at nitrogen atom of neighbouring molecule. Thus the intramolecular and intermolecular exchange interactions are comparable to each other in fine-crystalline sample of complex **6**. So, the uniform chain model ($H = -2J\,\Sigma S_iS_{i+1}$) was found to be more suitable than the exchange coupled dimer one for description of experimental data. The optimal values of exchange interaction parameters are: J = -8.0 (±0.2) K, g = 2.00 (±0.01).

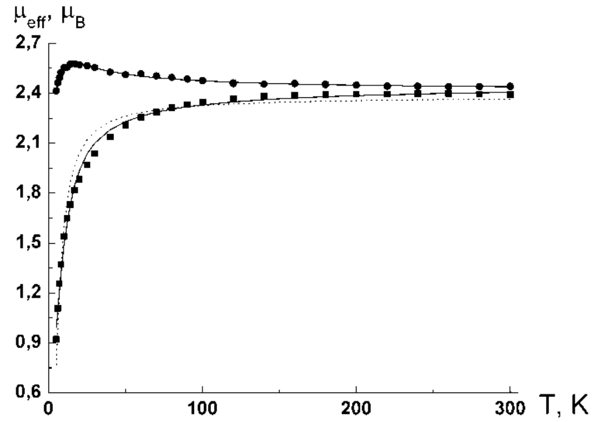

Fig. 5. The temperature dependences of μ_{eff} for complexes **6** (■) and **7** (●). Solid and dotted lines are theoretical curves. For complex **6** (■) the solid line was obtained by approximation using model of exchange coupled chain, the dotted line –exchange coupled dimer.

The value of μ_{eff} for **7** increases gradually to 2.58 μ_B at 17 K and then decreases slightly to 2.41 μ_B at 5 K. Thus in contrast to complex **6** the compound **7** is characterized by domination of ferromagnetic exchange interactions between spins of two imSQ ligands. Decrease of μ_{eff} value near 5 K indicates the presence of weak intermolecular antiferromagnetic exchange interaction in solid sample of **7**. Estimation of exchange interaction parameters was carried out using the model of exchange coupled dimer. The optimal values of interaction parameters are: J = 12.9 (±0.3) K, zJ' = -1.3 (±0.1) K, g = 1.98 (±0.01). It is necessary to note that the similar diradical indium complex **3** demonstrates moderate antiferromagnetic exchange (J = – 39.9 (±0.2) K [9a]) between *o*-iminosemiquinolate centres. Thus, a change of the ground spin state occurs for the structural analogues **3** and **7** which is caused by the change of the apical substituent on the metal atom. The given fact will be a topic for further research.

Crystal structures of complexes 5-7.

The crystal and molecular structures of complexes **5-7** were examined using X-ray diffraction. The selected bond lengths and valence angels are given in Table 1. There are two independent molecules in the unit cell of **5** which differ by the chlorine atoms and TMEDA fragment positions relative to *o*-iminobenzosemiquinonato ligand. The bond lengths and angles in both molecules are similar and only one of them will be described below. As in **4** [10b], the indium atom in **5** has a distorted octahedral environment (Fig. 6). The octahedral base is formed by the O(1), N(1), N(3) and Cl(1) atoms while the N(2) and Cl(2) atoms occupy apical positions. The deviation of indium atom from O(1)N(1)N(3)Cl(1) base is 0.15 Å. The value of N(2)-In(1)-Cl(2) angle is 158.24(11)º.

Table 1. Selected bond lengths [Å] and angles [°] of complexes **5, 6** and **7**

Complex imSQInCl$_2$(TMEDA) (**5**)							
Bond lengths				Valence angles			
In(1)-O(1)	2.163(3)	C(6)-N(1)	1.337(6)	O(1)-In(1)-N(1)	75.69(13)	N(3)-In(1)-Cl(2)	85.50(11)
In(1)-N(1)	2.263(4)	C(1)-C(2)	1.432(7)	O(1)-In(1)-N(3)	92.04(14)	Cl(1)-In(1)-Cl(2)	102.57(6)
In(1)-Cl(1)	2.4063(14)	C(2)-C(3)	1.370(7)	N(1)-In(1)-N(3)	167.60(15)	O(1)-In(1)-N(2)	79.95(13)
In(1)-Cl(2)	2.4649(14)	C(3)-C(4)	1.421(7)	O(1)-In(1)-Cl(1)	165.97(10)	N(1)-In(1)-N(2)	99.96(14)
In(1)-N(2)	2.512(4)	C(4)-C(5)	1.357(7)	N(1)-In(1)-Cl(1)	96.65(11)	N(3)-In(1)-N(2)	75.68(15)
In(1)-N(3)	2.363(4)	C(5)-C(6)	1.434(7)	N(3)-In(1)-Cl(1)	94.97(11)	Cl(1)-In(1)-N(2)	90.03(10)
C(1)-O(1)	1.295(6)	C(1)-C(6)	1.472(7)	O(1)-In(1)-Cl(2)	90.07(10)	Cl(2)-In(1)-N(2)	158.24(11)
				N(1)-In(1)-Cl(2)	96.16(11)		
Complex imSQ$_2$InSS (**6**)							
In(1)-O(1)	2.1700(10)	C(2)-C(3)	1.372(2)	O(2)-In(1)-O(1)	87.63(4)	N(2)-In(1)-S(1)	98.79(3)
In(1)-N(1)	2.2561(12)	C(3)-C(4)	1.437(2)	O(2)-In(1)-N(2)	74.35(4)	N(1)-In(1)-S(1)	101.31(3)
In(1)-O(2)	2.1688(10)	C(4)-C(5)	1.362(2)	O(1)-In(1)-N(2)	86.02(4)	O(2)-In(1)-S(2)	103.85(3)
In(1)-N(2)	2.2517(12)	C(5)-C(6)	1.425(2)	O(2)-In(1)-N(1)	87.29(4)	O(1)-In(1)-S(2)	166.12(3)
In(1)-S(1)	2.5606(4)	C(1)-C(6)	1.460(2)	O(1)-In(1)-N(1)	74.32(4)	N(2)-In(1)-S(2)	104.41(3)
In(1)-S(2)	2.5705(4)	C(27)-C(28)	1.428(2)	N(2)-In(1)-N(1)	153.68(4)	N(1)-In(1)-S(2)	98.13(3)
C(1)-O(1)	1.2928(18)	C(28)-C(29)	1.373(2)	O(2)-In(1)-S(1)	170.41(3)	S(1)-In(1)-S(2)	70.972(14)
C(6)-N(1)	1.3390(19)	C(29)-C(30)	1.425(2)	O(1)-In(1)-S(1)	98.72(3)		
C(27)-O(2)	1.2972(17)	C(30)-C(31)	1.364(2)				
C(32)-N(2)	1.3355(18)	C(31)-C(32)	1.421(2)				
C(1)-C(2)	1.434(2)	C(27)-C(32)	1.466(2)				
Complex imSQ$_2$InEt (**7**)							
In(1)-O(1)	2.1836(17)	C(3)-C(4)	1.430(4)	C(53)-In(1)-N(1)	122.59(10)	O(1)-In(1)-O(2)	149.07(7)
In(1)-N(1)	2.177(2)	C(4)-C(5)	1.362(4)	C(53)-In(1)-O(1)	106.36(8)	C(53)-In(1)-N(2)	118.60(10)
In(1)-O(2)	2.1874(17)	C(5)-C(6)	1.421(4)	N(1)-In(1)-O(1)	75.16(7)	N(1)-In(1)-N(2)	118.80(8)
In(1)-N(2)	2.192(2)	C(1)-C(6)	1.457(3)	C(53)-In(1)-O(2)	104.52(9)	O(1)-In(1)-N(2)	88.70(7)
In(1)-C(53)	2.157(3)	C(27)-C(28)	1.438(4)	N(1)-In(1)-O(2)	89.73(7)	O(2)-In(1)-N(2)	74.98(7)
C(1)-O(1)	1.297(3)	C(28)-C(29)	1.379(4)				
C(6)-N(1)	1.345(3)	C(29)-C(30)	1.442(4)				
C(27)-O(2)	1.289(3)	C(30)-C(31)	1.357(4)				
C(32)-N(2)	1.352(3)	C(31)-C(32)	1.421(4)				
C(1)-C(2)	1.434(4)	C(27)-C(32)	1.456(4)				
C(2)-C(3)	1.370(4)						

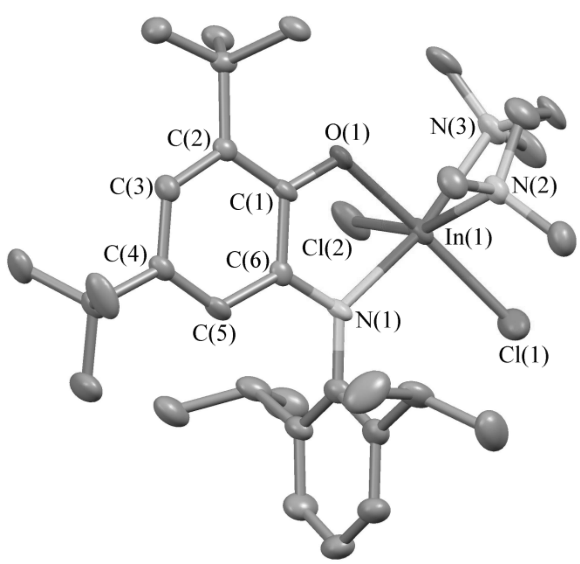

Fig. 6. The molecular structure of **5** with 50% thermal probability ellipsoids. The H atoms are omitted for clarity.

The values of In(1)-N(2) (2.512(4) Å) and In(1)-N(3) (2.363(4) Å) distances exceed the sum of covalent radii of these elements (2.17 Å [13]) but less than the sum of Van der Waals radii (4.2 Å [13]), thus these bonds have donor-acceptor nature.

It should be noted that the In(1)-N(3) bond is shorter than the In(1)-N(2). The same situation is observed for In-Cl bonds where the In(1)-Cl(1) distance (2.4063(14) Å) is less than the In(1)-Cl(2) (2.4649(14) Å). It is caused by the location of Cl(2) and N(3) atoms in the apical positions. The In(1)-N(2) and In(1)-Cl(2) bonds are orthogonal to the imSQ ligand plane and these Cl(2) and N(3) atoms participate in the hyperfine interaction with unpaired electron that is shown in the hyperfine structure of the EPR spectrum of **5**.

In accordance with X-ray diffraction data (Fig. 7) the coordination polyhedron of indium atom in **6** is a distorted octahedron. The O(1), O(2), S(1) and S(2) atoms form the octahedron base while the N(1) and N(2) atoms occupy apical sites. The *o*-iminoquinolate ligands are located in such a way where the nitrogen atoms are in *trans*-positions and the N(1)-In(1)-N(2) angle is 153.68(4)º. The $C_6H_2O(1)N(1)$ and $C_6H_2O(2)N(2)$ planes form the dihedral angle 53.02º.

There are two crystallographically unique molecules in the crystal cell of **7**. These molecules differ from each other by relative positions of ethyl groups and two redox active ligands.
The presence of two asymmetric chelate imSQ ligands in five-coordinating complex causes the chirality of metal centre and appearance of several isomers. This situation was previously observed for pentacoordinated indium and tin complexes based on imQ ligand [10a, 7h].

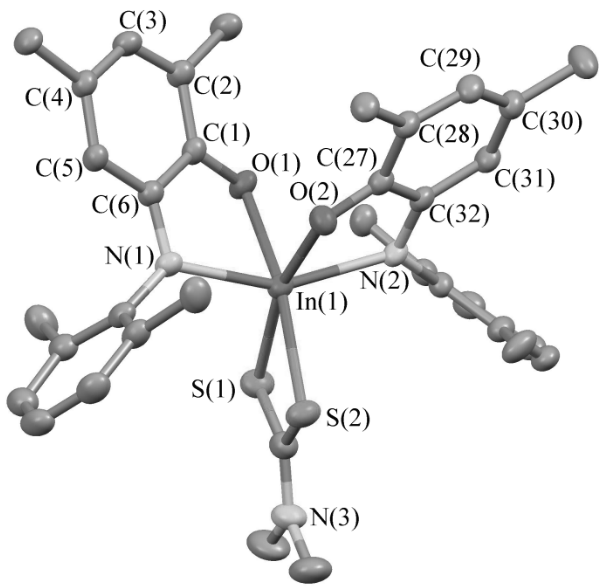

Fig. 7. The molecular structure of **6** with 50% thermal probability ellipsoids. The H atoms, methyl groups of *tert*-butyl and *iso*-propyl substituents are omitted for clarity.

The crystal cell of **7** contains the solvate molecule of with the ratio "complex : solvent" as 2 : 1.5. The coordination polyhedron is a distorted trigonal bipyramid (Fig. 8). The N(1), N(2) and C(53) atoms lie in the bipyramid base and O(1), O(2) atoms occupy apical sites. The O(1)-In(1)-O(2) angle is 149.07(7)º, the indium atom is neatly located in the N(1)N(2)C(53) plane. As in complex **6**, the arrangement of redox active ligands results in *trans*-position of the nitrogen atoms. The dihedral angle between $C_6H_2O(1)N(1)$ and $C_6H_2O(2)N(2)$ planes is 44.47º.

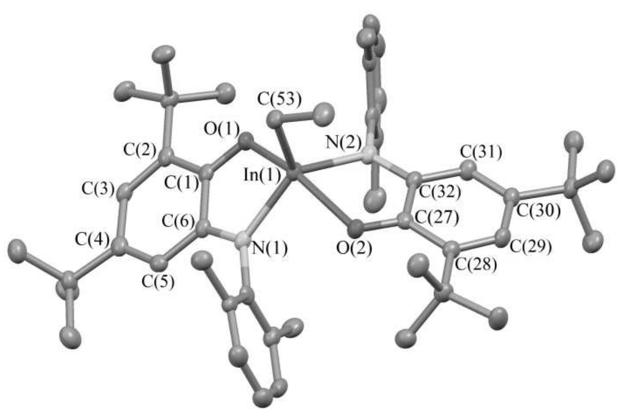

Fig. 8. The molecular structure of **7** with 50% thermal probability ellipsoids. The H atoms, methyl groups of *iso*-propyl substituents are omitted for clarity.

The geometries of imSQ ligands in **5-7** are typical for radical anion form of such type redox-active ligand and comparable with those in known *o*-iminobenzosemiquinonato metal complexes [14]. Thus the C(1)-O(1) and C(6)-N(1) bond lengths have intermediate value between values characteristic for corresponding single and double bonds. The In(1)-O(1) and In(1)-N(1) distances are equal or exceed slightly the sums of covalent radii of corresponding elements (2.16 Å for In-O and 2.17 Å for In-N [13]) and typical for radical anion form of imQ ligand coordination in previously reported indium derivatives [9]. The *o*-quinone alternation in six-membered C(1)-C(6) carbon ring is also observed. It appears in the separation of shorter C(2)-C(3) and C(4)-C(5) (1.357(7)-1.370(7) Å) bonds by longer C(1)-C(2), C(3)-C(4), C(5)-C(6) and C(1)-C(6) (1.421(7)-1.472(7) Å) bonds.

The evaluation of steric hindrances in the metal coordination sphere of indium *o*-iminosemiquinolate derivatives.

Mono-*o*-iminobenzosemiquinonato indium(III) compounds are unstable and undergo subsequent symmetrization with the formation of biradical products in most cases as it was shown above. Notably, in contrast to indium imQ derivatives described herein, the symmetrization of related mono-*o*-benzosemiquinonato indium(III) complexes leads mainly to the triradical compound $(3,6\text{-SQ})_3In$ (3,6-SQ is radical anion form of 3,6-di-tert-butyl-*o*-benzoquinone) [9].

The sterical situation in coordination sphere of metal is known to be one of the factors determining the final structure. Therefore we carried out the quantitative estimation of the shielding of the central metal atom based on the ligand solid angle approach (G-parameter [15]) for intermediate and resulting complexes. Previously, this approach allowed to explain the formation, stability and reactivity of a number of coordination compounds [16] including *o*-iminosemiquinonates [8d]. The geometric characteristics necessary for calculation of G-parameter were taken from X-ray diffraction data for $imSQ_2InI$ (**3**) [10a], $imSQInI_2$(TMEDA) (**4**) [10b], $imSQInCl_2$(TMEDA) (**5**), $imSQ_2InSS$ (**6**), $imSQ_2InEt$ (**7**). The geometry of unstable intermediate derivatives was optimized using DFT calculations. Calculations were performed at the B3LYP/3-21G level. Additional calculations of G-parameters for optimized geometries of **3-7** were made in order to evaluate the adequacy of the chosen level of theory. It is seen (Table 2) that the calculated structural parameters are in good agreement with experimental.

Table 2. The percentage of the metal coordination sphere shielded by all ligands (G-parameter) for indium(III) complexes. G-parameters for **3-7** based on X-ray data are presented in square brackets.

Complex	G, %	Complex	G, %
3	85.7(2) [86.9(2)]	**11**	65.1(2)
4	89.6(2) [91.3(2)]	**12**	66.4(2)
5	88.7(2) [88.9(2)]	**13**	76.1(2)
6	90.2(2) [90.7(2)]	$imSQ_2InCl$	85.8(2)
7	87.6(2) [87.4(2)]	$imSQInI_2$	65.0(2)
imSQInI(SS)	74.9(2)	imSQInI(Et)(TMEDA)	91.2(2)
10	81.3(2)		

The oxidation of **1** with O_2, I_2 and $HgCl_2$ leads to the formation of stable compounds $imSQ_2InI$ (**3**), $imSQInI_2$(TMEDA) (**4**) and $imSQInCl_2$(TMEDA) (**5**) respectively. The values of G-parameter for these isolated products are in a fairly narrow range 86-90 %.

As mentioned above we were unable to unambiguously determine the composition of mono-*o*-iminobenzosemiquinonato indium(III) specie formed as the result of oxidation of **1** with TMUDS. The modeling of the geometric parameters for imSQInI(SS)(TMEDA) (**8**) complex as sum of ligand solid angels has shown that the saturation of the metal coordination sphere by ligands exceeds 100 %, i.e. the seven-coordinated species should not exist in such a form (Scheme 4). Possibly it loses the TMEDA molecule that leads to the coordinatively unsaturated (G = 74.9(2) %) and unstable imSQInI(SS) species. Thus the monoradical indium(III) derivative should undergo symmetrization to form the stable product. Two ways of symmetrization are possible (Scheme 4). The first one leads to complex $imSQ_2InI$ (**3**) and the second one – to $imSQ_2InSS$ (**6**). In the accordance with values of G-parameter, both these compounds can be stable and the choice of symmetrization way is probably determined by the solubility of second products ($IInSS_2$ and I_2InSS) (Scheme 4).

The reason of symmetrization of monoradical complex $imSQInSS_2$ (**10**) (G = 81.3(2) %) is also its coordination unsaturation and **10** transforms into $imSQ_2InSS$ (**6**).

The intermediate mono-*o*-iminobenzosemiquinonato indium(III) derivatives **11-13** are characterized by low G-parameters that causes their symmetrization too (Scheme 5).

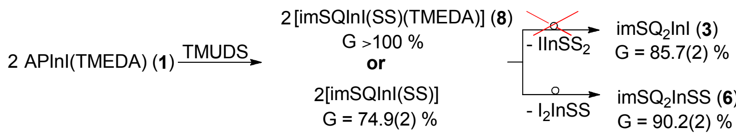

Scheme 4. The stages of reaction of APInI(TMEDA) (**1**) with TMUDS

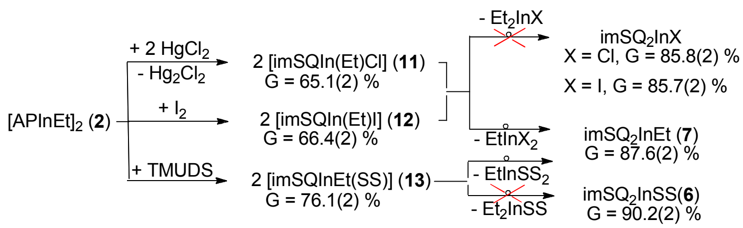

Scheme 5. The stages of oxidation of $[APInEt]_2$ (**2**) with $HgCl_2$, I_2 and TMUDS

There are two ways of symmetrization for unstable compounds **11-13**. The first one leads to $imSQ_2InEt$ (**7**). The second one results in the formation of $imSQ_2InX$ (X is Cl or I) in the case of **11** and **12** or $imSQ_2InSS$ (**6**) in the case of **13**. All these biradical indium(III) derivatives are stable (G-parameters are in the range 86-90 %). The formation of complex **7** as the final product of symmetrization of **11-13** (Scheme 5) can be explained by the lower solubility of co-products $EtInX_2$ *vs.*Et_2InX and $EtInSS_2$ *vs.*Et_2InSS. The precipitation of the monoalkylindium derivatives promotes the formation of **7**.

We have analyzed additional model compound $imSQInI_2$. It is known that the reaction of equimolar amounts of imSQNa with InI_3 leads to the formation of $imSQ_2InI$ (**3**) as the result of symmetrization of monoradical complex $imSQInI_2$ [10a]. The tetracoordinated compound has G-parameter equal to 65.0(2) % and is unstable.

Conclusions

In summary, in the course of present study it was found that the oxidation of indium *o*-amidophenolate complexes **1** and **2** proceeds through the formation of monoradical *o*-iminobenzosemiquinonato metal derivatives **8,10-13** which can be detected in solutions using EPR. In most cases such intermediate indium(III) species undergo the symmetrization due to their coordination unsaturation that leads to the corresponding stable biradical complexes. The executed calculations of the percentage of the metal coordination sphere shielded by all ligands (G-parameter) for series of indium(III) *o*-iminobenzosemiquinonato complexes described in this report indicates that the optimal values of G-parameter for stable derivatives are in the range of 86-90 %.

Experimental

Experimental Details

All reactants were purchased from Aldrich. Solvents were purified by standard methods [17]. The following reactants sodium *o*-iminobenzosemiquinolate imSQNa [10a], InI [18], **1**, **2** [10b] and I_2InEt [19] were prepared according to the known procedures. All manipulations on complexes were performed in vacuum under conditions in which oxygen and moisture were excluded.

The infrared spectra of complexes in the 4000–400 cm^{-1} range were recorded on a FSM 1201 Fourier-IR spectrometer in nujol. EPR spectra were recorded by using a Bruker EMX spectrometer (working frequency ≈ 9.75 GHz). The g_i values were determined using 2,2-diphenyl-1-picrylhydrazyl (DPPH) as the reference (g_i=2.0037). EPR spectra were simulated with the WinEPR SimFonia Software (Bruker). The elemental analysis was performed on an Elemental Analyzer Euro EA 3000 instrument.

The magnetic susceptibility of the polycrystalline complexes was measured with a Quantum Design MPMS*XL* SQUID magnetometer in the temperature range 2-300 K with magnetic field of up to 5 kOe. None of complexes exhibited any field dependence of molar magnetization at low temperatures. Diamagnetic corrections were made using the Pascal constants. The effective magnetic moment was calculated as $\mu_{eff}(T) = [(3k/N_A\mu_B^2)\chi T]^{1/2} \approx (8\chi T)^{1/2}$.

The oxidation of 1 with dioxygen.

The solution of complex **1** (0.35 g, 0.47 mmol) in THF (25 ml) was exposed to the fixed volume of dry dioxygen (50 ml). The reaction mixture was stirred for few minutes during that the color changed from orange to deep green. The THF was replaced with hexane (15 ml). The crystalline product $imSQ_2InI$ (**3**) was isolated from the reaction mixture after storage of the later at -18ºC overnight. The total yield of analytically pure compound is 0.14 g (58 %).

The oxidation of 1 with iodine.

The solution of complex **1** (0.35 g, 0.47 mmol) in THF (25 ml) was added to the solution of I_2 (0.0596 g, 0.235 mmol) in the same solvent (3 ml). The reaction mixture turned brown. The THF was removed under reduced pressure. The solid residue was dissolved in diethyl ether (15 ml). The solution was stored at -18ºC overnight. It led to the formation of brown-green crystals of $imSQInI_2$(TMEDA) (**4**). The total yield of analytically pure compound is 0.27 g (61 %).

The interaction of 1 with $HgCl_2$.

The solution of complex **1** (0.35 g, 0.47 mmol) in THF (25 ml) was added to the solution of $HgCl_2$ (0.1276 g, 0.47 mmol) in the same solvent (5 ml). The reaction mixture was stirred during 15-20 minutes. The solution color gradually changed from orange to deep blue. The THF was replaced by hexane (15 ml). The white-yellow precipitate of Hg_2I_2 was removed by filtration. The following storage of the solution at -18ºC during few hours led to the formation of crystalline blue-green product $imSQInCl_2$(TMEDA) (**5**). The total yield of analytically pure compound is 0.21 g (65 %).

Anal. Calc. for $C_{32}H_{53}Cl_2InN_3O$: C, 56.40; H, 7.84; Cl, 10.40; In, 16.85%. Found: C, 56.67; H, 7.95; Cl, 10.34; In, 16.49 %. IR (Nujol, KBr) cm^{-1}: 1588 (w), 1442 (s), 1426 (s), 1407 (m), 1364 (m), 1351 (m), 1327 (m), 1319 (m), 1306 (w), 1288 (w), 1270 (w), 1252 (m), 1213 (m), 1198 (w), 1181 (w), 1164 (w), 1124 (w), 1120 (w), 1102 (w), 1056 (w), 1046 (w), 1024 (m), 1011 (m), 992 (w), 952 (m), 937 (w), 913 (w), 888 (w), 866 (m), 817 (w), 797 (s), 772 (m), 768 (m), 743 (w), 707 (w), 667 (w), 644 (w), 623 (w), 610 (w), 589 (w), 574 (w), 539 (w), 529 (w), 497 (w), 478 (w).

The oxidation of 1 with TMUDS.

The solution of **1** (0.35 g, 0.47 mmol) in THF (25 ml) was added to the solution of TMUDS (0.0565 g, 0.235 mmol) in the same solvent (5 ml). The reaction mixture was stirred during 15-20 minutes at 40-50ºC. The solution color changed from orange to deep green. The THF was removed under reduced pressure. The solid residue was dissolved in hexane (15 ml). The obtained solution was kept during an hour, the formation of white precipitate was observed. The solution was separated from I_2InSS by filtration and stored at -18ºC overnight. The deep green crystals of $imSQ_2InSS$ (**6**) were obtained as the result. The total yield of analytically pure compound is 0.16 g (69 %).

Anal. calc. for $C_{55}H_{80}InN_3O_2S_2$: C, 66.44; H, 8.11; In, 11.55; S, 6.45 %. Found: C, 66.79; H, 8.26; In, 11.40; S, 6.21 %. IR (Nujol, KBr) cm^{-1}: 1585 (m), 1510 (m), 1444 (s), 1430 (s), 1412 (m), 1362 (s), 1352 (s), 1330 (s), 1323 (m), 1307 (m), 1267 (w), 1251 (s), 1216 (w), 1198 (m), 1167 (m), 1136 (w), 1113 (w), 1098 (w), 1055 (w), 1042 (w), 1026 (w), 992 (w), 979 (m), 936 (w), 924 (w), 910 (w), 884 (w), 866 (m), 822 (w), 803 (m), 797 (m), 776 (w), 772 (w), 763 (w), 744 (w), 705 (w), 665 (w), 646 (w), 626 (w), 604 (w), 571 (w), 538 (w), 528 (w), 496 (w), 476 (w), 463 (w).

The exchange interaction of imSQNa with $IInSS_2$.

The preparation of $IInSS_2$. The solution of TMUDS (0.3 g, 1.25 mmol) in THF (20 ml) was added to the suspension of InI (0.151 g, 0.625 mmol) in the same solvent (5 ml). The reaction mixture was stirred until full disappearance of the red precipitate InI and the formation of clear solution. The solution was concentrated (5 ml) and hexane was added dropwise. The white precipitate $IInSS_2$ was separated from solution by filtration. The total yield of analytically pure compound is 0.26 g (86 %).

Anal. calc. for $C_6H_{12}IInN_2S_4$: C, 14.95; H, 2.51; I, 26.32; In, 23.81; S, 26.60. Found: C, 15.13; H, 2.75; I, 26.18; In, 23.76; S, 26.41.

The solution of imSQNa (0.4 g, 0.994 mmol) in THF (25 ml) was added to the solution of $IInSS_2$ (0.479 g, 0.994 mmol) in the same solvent (10 ml). The reaction mixture turned deep green. The THF was replaced by hexane (15 ml). The solution was kept during an hour at room temperature and the formation of white precipitate $InSS_3$ [20] was observed. The precipitate was removed by filtration. The resulted solution was stored at -18ºC overnight that led to the formation of crystalline product $imSQ_2InSS$ (**6**). The total yield of analytically pure compound is 0.28 g (57 %).

The oxidation of $[APInEt]_2$ (2) with $HgCl_2$.

The solution of **2** (0.35 g, 0.334 mmol) in THF (20 ml) was added to the solution of $HgCl_2$ (0.1814 g, 0.668 mmol) in the same solvent (10 ml). The reaction mixture was stirred during 15-20 minutes at room temperature. The color changed from orange to deep green and the precipitation of Hg_2Cl_2 was observed. The deposit was removed by filtration. The THF was replaced by hexane (15 ml). The reaction mixture was kept during an hour at ambient temperature and the precipitation of $EtInCl_2$ was observed. The $EtInCl_2$ was removed by filtration. The following storage of the solution at -18ºC led to formation of crystalline product $imSQ_2InEt$•0.75(hexane) (**7**•0.75(hexane)). The total yield of analytically pure compound is 0.17 g (53 %).

Anal. calc. for $C_{58.5}H_{89.5}InN_2O_2$: C, 72.61; H, 9.32; In, 11.87 %. Found: C, 72.86; H, 9.55; In, 11.62. IR (Nujol, KBr) cm^{-1}: 1588 (s), 1467 (s), 1442 (s), 1435 (s), 1360 (s), 1355 (s), 1334 (s), 1320 (m), 1255 (s), 1214 (w), 1198 (m), 1170 (m), 1112 (m), 1102 (m), 1056 (m), 1042 (w), 1026 (m), 1009 (w), 992 (m), 880 (w), 873 (m), 861 (m), 820 (w), 797 (s), 779 (w), 764 (m), 744 (w), 709 (w), 665 (w), 648 (w), 638 (m), 626 (w), 607 (w), 585 (w), 574 (w), 539 (w), 527 (w), 497 (w), 477 (w).

The oxidation of $[APInEt]_2$ (2) with I_2.

The solution of **2** (0.35 g, 0.334 mmol) in THF (20 ml) was added to the solution of I_2 (0.0848 g, 0.334 mmol) in the same solvent (5 ml). The reaction mixture turned deep green. The replacement of THF by hexane (15 ml) led to the formation of $EtInI_2$ deposit. The solution was kept during an hour and separated from $EtInI_2$ by filtration. The result product $imSQ_2InEt$•0.75(hexane) (**7**•0.75(hexane)) was isolated according to the method described

Table 3. Summary of crystal and refinement data for complexes **5**, **6** and **7**•0.75(DME)

Complex	imSQInCl$_2$(TMEDA) (**5**)	imSQ$_2$InSS (**6**)	imSQ$_2$InEt•0.75(DME) (**7**•0.75(DME))
Empirical formula	$C_{32}H_{53}Cl_2InN_3O$	$C_{55}H_{80}InN_3O_2S_2$	$C_{57}H_{86.50}InN_2O_{3.50}$
Formula weight	681.49	994.16	970.60
Temperature [K]	150(2)	150(2)	100(2)
Wavelength [Å]	0.71073	0.71073	0.71073
Crystal system	Monoclinic	Triclinic	Monoclinic
Space group	P2(1)/n	P-1	P2(1)/n
Unit cell dimensions [Å] [°]	a = 11.7294(9) b = 17.9283(13) c = 32.527(2) α = 90 β = 96.017(2) γ = 90	a = 11.8378(8) b = 13.5406(9) c = 17.8321(11) α = 101.5320(10) β = 92.0740(10) γ = 99.2270(10)	a = 20.5030(6) b = 22.1273(6) c = 25.5483(7) α = 90 β = 106.8230(10) γ = 90
Volume [Å^3]	6802.3(9)	2757.5(3)	11094.6(5)
Z	8	2	8
Density (calculated) [g/cm^3]	1.331	1.197	1.162
Absorption coefficient [mm^{-1}]	0.880	0.544	0.468
Crystal size [mm^3]	0.40 x 0.27 x 0.15	0.57 x 0.26 x 0.15	0.27 x 0.26 x 0.21
Theta range for data collection [°]	1.79 to 26.00	1.74 to 27.00	1.84 to 26.00
Reflections collected	39470	25742	94144
Independent reflections	13342	11942	21728
R(int)	0.0692	0.0194	0.0768
Completeness to theta max	99.7	99.3	99.5
Absorption correction	Semi-empirical from equivalents	Semi-empirical from equivalents	Semi-empirical from equivalents
Max. and min. transmission	0.8794 and 0.7199	0.9229 and 0.7468	0.9081 and 0.8840
Refinement method	Full-matrix least-squares on F^2	Full-matrix least-squares on F^2	Full-matrix least-squares on F^2
Data / restraints / parameters	13342 / 0 / 731	11942 / 0 / 590	21728 / 58 / 1211
Final R indices [I>2sigma(I)]	R1 = 0.0647 wR2 = 0.1331	R1 = 0.0315 wR2 = 0.0772	R1 = 0.0537 wR2 = 0.1223
R indices (all data)	R1 = 0.0984 wR2 = 0.1432	R1 = 0.0385 wR2 = 0.0801	R1 = 0.0879 wR2 = 0.1344
Goodness-of-fit on F^2	1.073	1.073	1.004
Largest diff. peak and hole [e/Å^3]	2.752 and -1.115	0.737 and -0.437	1.583 and -0.699

above. The total yield of analytically pure compound is 0.21 g (65 %).

The oxidation of [APInEt]$_2$ (2) with dioxygen.

The solution of **2** (0.35 g, 0.334 mmol) in THF (20 ml) was exposed to dry dioxygen (50 ml). The reaction mixture turned deep green during few minutes. The THF was replaced with hexane (15 ml). The result complex imSQ$_2$InEt•0.75(hexane) (**7**•0.75(hexane)) was isolated according to the method described above. The total yield of analytically pure compound is 0.20 g (62 %).

The interaction of [APInEt]$_2$ (2) with TMUDS.

The solution of **2** (0.35 g, 0.334 mmol) in THF (20 ml) was added to the solution of TMUDS (0.08 g, 0.334 mmol) in the same solvent (7 ml). The reaction mixture was stirred during 15-20 minutes at 40-50ºC. The solution color changed from pale yellow to deep green. The THF was removed under reduced pressure and the solid residue was dissolved in hexane (15 ml). The reaction mixture was kept during an hour and the formation of white precipitate EtInSS$_2$ was observed. The precipitate was removed by filtration. The resulting complex imSQ$_2$InEt•0.75(hexane) (**7**•0.75(hexane)) was isolated according to the method described above. The total yield of analytically pure compound is 0.20 g (60 %).

X-ray crystallographic studies of imSQInCl$_2$(TMEDA) (5), imSQ$_2$InSS (6) and imSQ$_2$InEt•0.75(DME) (7•0.75(DME)).

The single crystals suitable for X-ray diffraction analysis were obtained from hexane (for **5** and **6**) or DME (for **7**·0.75(DME)). The intensity data were collected at 150 K (for **5** and **6**) and 100 K (for **7**·0.75(DME)) on a Smart Apex diffractometer with graphite monochromated Mo-K$_\alpha$ radiation (λ = 0.71073 Å) in the φ-ω scan mode (ω = 0.3°, 10 sec on each frame). The intensity data were integrated by SAINT program [21]. SADABS [22] was used to perform area-detector scaling and absorption corrections. The structures were solved by direct methods and were refined on

F^2 using all reflections with SHELXTL package [23]. All non-hydrogen atoms were refined anisotropically. The hydrogen atoms were placed in calculated positions and refined in the "riding-model". Selected bond lengths and angles of complexes are given in Table 1. Table 3 summarises the crystal data and some details of the data collection and refinement.

Crystallographic data for the structural analysis have been deposited with the Cambridge Crystallographic Data Centre, CCDC № 1002475-1002477 for compounds **5-7**. Copies of this information may be obtained free of charge from The Director, CCDC, 12, Union Road, Cambridge CB2 1EZ, UK (fax: +44 1223 336033; e-mail: deposit@ccdc.cam.ac.uk or www: http://www.ccdc.cam.ac.uk).

Density functional theory calculations.

DFT calculations were performed with the GAUSSIAN 03 [24] program package using the B3LYP/3-21G level of theory. The absence of imaginary frequencies after the optimization procedure suggests that the molecular geometries correspond to the energy minima.

Acknowledgements

We are grateful to the Russian Scientific Foundation (grant 14-03-01296) for financial support of this work.

Notes and references

[a] *G.A. Razuvaev Institute of Organometallic Chemistry Russian Academy of Sciences, Tropinina Street 49, 603950 Nizhniy Novgorod, GSP-445, Russian Federation.*
Fax: (+7) 831-462-74-97; E-mail : pial@iomc.ras.ru
[b] *N.I. Lobachevsky Nizhny Novgorod State University, 23 Gagarin Avenue, 603950 Nizhny Novgorod, Russian Federation*
[c] *International Tomography Center, Siberian Branch, Russian Academy of Sciences, Institutskaya Street 3a, 630090 Novosibirsk, Russian Federation*

1 (a) G.A. Abakumov, A.I. Poddel'sky, E.V. Grunova, V.K. Cherkasov, G.K. Fukin, Yu.A. Kurskii and L.G. Abakumova, *Angew. Chem. Int. Ed.*, 2005, **44**, 2767-2771; (b) V.K. Cherkasov, G.A. Abakumov, E.V. Grunova, A.I. Poddel'sky, G.K. Fukin, E.V. Baranov, Yu.A. Kursky and L.G. Abakumova, *Chem. Eur. J.*, 2006, **12**, 3916-3927; (c) A.I. Poddel'sky, Y.A. Kuskii, A.V. Piskunov, N.N. Somov, V.K. Cherkasov and G.A. Abakumov, *Applied Organomet. Chem.*, 2011, **25**, 180-189.

2 E.V. Ilyakina, A.I. Poddel'sky, V.K. Cherkasov and G.A. Abakumov, *Mendeleev Commun.*, 2012, **22**, 208-210.

3 I.L. Fedushkin, A.S. Nikipelov and K.A. Lyssenko, *J. Am. Chem Soc.*, 2010, **132**, 7874–7875.

4 (a) A.V. Piskunov, I.N. Meshcheryakova, G.K. Fukin, A.S. Shavyrin, V.K. Cherkasov and G.A. Abakumov, *Dalton Trans.*, 2013, **42**, 10533-10539; (b) A.V. Piskunov, I.V. Ershova, G.K. Fukin and A.S. Shavyrin, *Inorg. Chem. Commun.*, 2013, **38**, 127-130.

5 (a) W.I. Dzik, J.I. van der Vlugt, J.N.H. Reek and B. de Bruin, *Angew. Chem. Int. Ed.*, 2011, **50**, 3356-3358; (b) I.L. Fedushkin, A.S. Nikipelov, A.G. Morozov, A.A. Skatova, A.V. Cherkasov and G.A. Abakumov, *Chem. Eur. J.*, 2012, **18**, 255-266; (c) P.J. Chirik, K. Wieghardt, *Science*, 2010, **327**, 794-795; (d) O.R. Luca, R.H. Crabtree, *Chem. Soc. Rev.*, 2013, **42**, 1440-1459.

6 (a) C.G. Pierpont, *Coord. Chem. Rev.*, 2001, **219 – 221**, 415-433; (b) C.G. Pierpont, *Coord. Chem. Rev.*, 2001, **216 – 217**, 99-125; (c) A.I. Poddel'sky, V.K. Cherkasov and G.A. Abakumov, *Coord. Chem. Rev.*, 2009, **253**, 291-324; (d) W. Kaim, *Inorg. Chem.*, 2011, **50**, 9752–9765; (e) N. Deibel, D. Schweinfurth, S. Hohloch, J. Fiedler, B. Sarkar, *Chem. Commun.*, 2012, **48**, 2388-2390; (f) E.M. Matson, S.M. Franke, N.H. Anderson, T. D. Cook, P.E. Fanwick, S.C. Bart, *Organometallics*, 2014, **33**, 1964–1971; (g) D. Das, H. Agarwala, A.D. Chowdhury, T. Patra, S.M. Mobin, B. Sarkar, W. Kaim, G.K. Lahiri, *Chem. Eur. J.*, 2013, **19**, 7384–7394; (h) S. Ghorai, C. Mukherjee, *Chem. Commun.*, 2012, **48**, 10180–10182; (i) S.E. Balaghi, E. Safaei, L. Chiang, E.W.Y. Wong, D. Savard, R.M. Clarke T. Storr, *Dalton Trans.*, 2013, **42**, 6829; (j) N. Deibel, D. Schweinfurth, S. Hohloch, M. Delor, I.V. Sazanovich, M. Towrie, J.A. Weinstein, B. Sarkar, *Inorg. Chem.*, 2014, **53**, 1021−1031; (k) A.H. Randolph, N.J. Seewald, K.Rickert, S.N. Brown, *Inorg. Chem.*, 2013, **52**, 12587–12598; (l) S. Sproules, R.R. Kapre, N. Roy, Th. Weyhermüller, K. Wieghardt, Inorg. Chim. Acta, 2010, **363,** 2702–2714.

7 (a) T.A. Annan, D.G. Tuck, *Can. J. Chem.*, 1989, **67**, 1807-1814; (b) H.E. Mabrouk, D.G. Tuck, *J. Chem. Soc., Dalton Trans*. 1988, 2539; (c) G.M. Barnard, M.A. Brown, H.E. Mabrouk, B.R. McGarvey and D.G. Tuck, *Inorg. Chim. Acta.*, 2003, **349**, 142-148; (d) A.V. Lado, A.I. Poddel'sky, A.V. Piskunov, G.K. Fukin, E.V. Baranov, V.N. Ikorskii, V.K. Cherkasov and G.A. Abakumov, *Inorg. Chim. Acta.*, 2005, **358**, 4443-4450; e) G.A. Abakumov, V.K. Cherkasov, A.V. Piskunov, A.V. Lado, G.K. Fukin and L.G. Abakumova, *Russ. Chem. Bull.*, 2006, **55**, 1146-1154; f) A.V. Lado, A.V. Piskunov, V.K. Cherkasov, G.K. Fukin and G.A. Abakumov, *Russ. J. Coord. Chem.*, 2006, **32**, 173-179; g) A.V. Piskunov, A.V. Lado, E.V. Ilyakina, G.K. Fukin, E.V. Baranov, V.K. Cherkasov and G.A. Abakumov, *J. Organomet. Chem.*, 2008, **693**, 128-134; h) A.V. Piskunov, I.N. Mescheryakova, G.K. Fukin, E.V. Baranov, M. Hummert, A.S. Shavyrin, V.K. Cherkasov and G.A. Abakumov, *Chem. Eur. J.*, 2008, **14**, 10085-10093; i) E.V. Ilyakina, A.I. Poddel'sky, A.V. Piskunov, N.V. Somov, V.K. Cherkasov and G.A. Abakumov, *Inorg. Chim. Acta.*, 2012, **380**, 57-64; j) E.V. Ilyakina, A.I. Poddel'sky, A.V. Piskunov, N.V. Somov, G.A. Abakumov and V.K. Cherkasov, *Inorg. Chim. Acta.*, 2013, **394**, 282-288; k) E.V. Ilyakina, A.I. Poddel'sky, A.V. Piskunov, G.K. Fukin, V.K. Cherkasov and G.A. Abakumov, *Z. Anorg. Allg. Chem.*, 2012, **638**, 1323-1327.

8 (a) G.A. Abakumov, V.A. Tsaryapkin, L.V. Gorbunova, V.K. Cherkasov and G.A. Razuvaev, *Russ. Chem. Bull.*, 1981, **30**, 157-161; (b) G.A. Razuvaev, G.A. Abakumov, P.Ya. Bayushkin, V.A. Tsaryapkin and V.K. Cherkasov, *Russ. Chem. Bull.*, 1984, **33**, 1915-1922; (c) M.A. Brown, B.R. McGarvey, A. Ozarowski and D.G. Tuck, *J. Organomet. Chem.*, 1998, **550**, 165–172; (d) A.V. Piskunov, I.N. Meshcheryakova, E.V. Baranov, G.K. Fukin, V.K. Cherkasov and G.A. Abakumov, *Russ. Chem. Bull.*, 2010, **59**, 361-370.

9 A.V. Piskunov, A.V. Maleeva, I.N. Meshcheryakova and G.K. Fukin, *Russ. J. Coord. Chem.*, 2013, **39**, 245–256.

10 (a) A.V. Piskunov, I.N. Mescheryakova, A.S. Bogomyakov, G.V. Romanenko, V. K. Cherkasov and G.A. Abakumov, *Inorg. Chem. Commun.*, 2009, **12**, 1067-1070; (b) A.V. Piskunov, I.N. Mescheryakova, G.K. Fukin, V.K. Cherkasov and G.A. Abakumov, *New J. Chem.*, 2010, **34**, 1746-1750.

11 Yu. Yu. Lur'e, Handbook of Analytical Chemistry, Khimia, Moscow, 1971, 454.

12 J. Emsley, The Elements, Clarendon Press, Oxford, 1991, 251.

13 S.S. Batsanov, *Russ. J. Inorg. Chem.*, 1991, **36**, 1694-1706.

14 S.N. Brown. *Inorg. Chem.*, 2012, **51**, 1251-1260.

15 (a) I.A. Guzei, M. Wendt, *Dalton. Trans.*, 2006, 3991-3999; (b) I.A. Guzei, M. Wendt, Program Solid-G, Madison, WI, USA, 2004.

16 (a) G.K. Fukin, I.A. Guzei and E.V. Baranov, *J. Coord. Chem.*, 2007, **60**, 937-944; (b) G.K. Fukin, I.A. Guzei and E.V. Baranov, *J. Coord. Chem.*, 2008, **61**, 1678-1688; (c) G.K. Fukin, I.A. Guzei, E.V. Baranov and G.A Domrachev, *Struct. Chem.*, 2009, **20**, 643-654; (d) G.K. Fukin, E.V. Baranov, A.I. Poddel'sky, V.K. Cherkasov and G.A. Abakumov, *ChemPhysChem.*, 2012, **13**, 3773-3776.

17 D.D. Perrin, W.L.F. Armarego, D.R. Perrin, *Purification of Laboratory Chemicals*, Pergamon, Oxford, 1980.

18 B.H. Freeland, D.G. Tuck, *Inorg. Chem.*, 1976, **15**, 475–476.

19 J.S. Poland, D.G. Tuck, *J. Organometal. Chem.*, 1972, **42**, 315-323.

20 L.C. Carvalho, M.M. Oliveira, C. Peppe, G.M. Pessoa, A.G. Souza and C. Airoldi, *Thermochimica Acta*, 1999, **328**, 223-230.

21 Bruker, SAINTPLUS Data Reduction and Correction Program v.6.02a, Bruker AXS, Madison, WI, USA, 2000.

22 G. M. Sheldrick, SADABS v.2.01, Bruker/Siemens Area Detector Absorption Correction Program, Bruker AXS, Madison, WI, USA, 1998.

23 G. M. Sheldrick, SHELXTL v.6.12, Structure Determination Software Suite, Bruker AXS, Madison, WI, USA, 2000.

24 M. J. Frisch, G. W. Trucks, H. B. Schlegel, M. J. Frisch, G. W. Trucks, H. B. Schlegel, G. E. Scuseria, M. A. Rob, J. R. Cheeseman, J. A. Montgomery, Jr., T. Vreven, K. N. Kudin, J. C. Burant, J. M. Millam, S. S. Iyengar, J. Tomasi, V. Barone, B. Mennucci, M. Cossi, G. Scalmani, N. Rega, G. A. Petersson, H. Nakatsuji, M. Hada, M. Ehara, K. Toyota, R. Fukuda, J. Hasegawa, M. Ishida, T. Nakajima, Y. Honda, O. Kitao, H. Nakai, M. Klene, X. Li, J. E. Knox, H. P. Hratchian, J. B. Cross, V. Bakken, C. Adamo, J. Jaramillo, R. Gomperts, R. E. Stratmann, O. Yazyev, A. J. Austin, R. Cammi, C. Pomelli, J. W. Ochterski, P. Y. Ayala, K. Morokuma, G. A. Voth, P. Salvador, J. J. Dannenberg, V. G. Zakrzewski, S. Dapprich, A. D. Daniels, M. C. Strain, O. Farkas, D. K. Malick, A. D. Rabuck, K. Raghavachari, J. B. Foresman, J. V. Ortiz, Q. Cui, A. G. Baboul, S. Clifford, J. Cioslowski, B. B. Stefanov, G. Liu, A. Liashenko, P. Piskorz, I. Komaromi, R. L. Martin, D. J. Fox, T. Keith, M. A. AlLaham, C. Y. Peng, A. Nanayakkara, M. Challacombe, P. M. W. Gill, B. Johnson, W. Chen, M. W. Wong, C. Gonzalez and J. A. Pople, *Gaussian 03, Revision A.1, Gaussian, Inc., Pittsburgh (PA),* 2003.